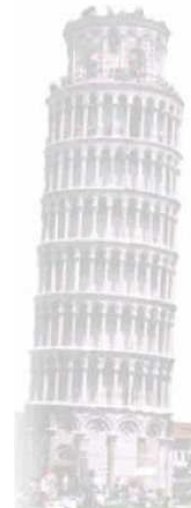
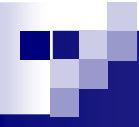


A Case Study: Detection of a Subspace Gaussian Target in K-Distributed Clutter



Fulvio GINI and Maria S. GRECO
Dept. of Ingegneria dell'Informazione
University of Pisa
Via G. Caruso 16, I-56122, Pisa, Italy
f.gini@ing.unipi.it, m.greco@ing.unipi.it

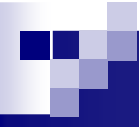




A Case Study: Subspace Gaussian Target

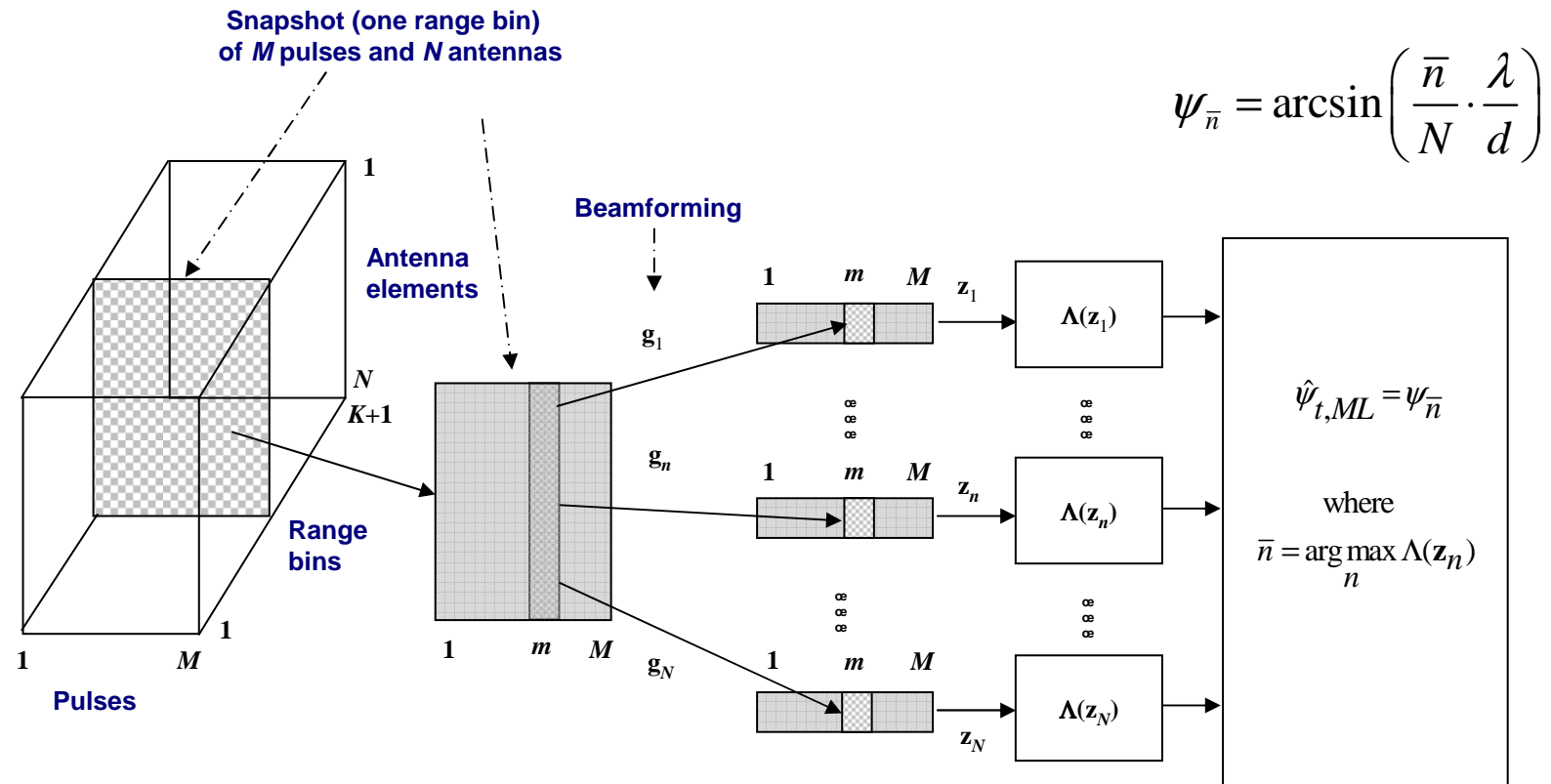
2

- In this 2nd part of the **case study** we investigate the performance of the optimum NP detector, the GLRT detector and the subspace CFAR detector in correlated **K-distributed clutter** with a-priori known normalized covariance matrix **M**.
- **Target:** subspace Gaussian target
- **Clutter:** correlated K-distributed clutter
- **Thermal noise:** negligible
- **Jammer:** absent



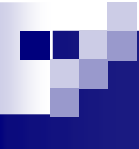
A Case Study: Subspace Gaussian Target

3



■ Block diagram of the Beam-Space Pre-Doppler detector [War94]

[War94] Ward J., "Space-time adaptive processing for airborne radar," *Tech. Rep. TR-1015*, Massachusetts Institute of Technology, Lincoln Labs, Cambridge, MA, December 1994.



A Case Study: Subspace Gaussian Target

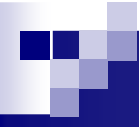
4

- The target signal at the output of the n th beamformer has been represented as

$$\mathbf{s}_t = \mathbf{H} \cdot \boldsymbol{\theta}, \quad \text{where } \mathbf{H} = \mathbf{U}_s \quad \text{and} \quad \boldsymbol{\theta} \sim \mathcal{CN}(\mathbf{0}, \sigma_\theta^2 \boldsymbol{\Lambda}_\theta)$$

$$\mathbf{R}_t = E\{\mathbf{s}_t \mathbf{s}_t^H\} = \mathbf{H} E\{\boldsymbol{\theta} \boldsymbol{\theta}^H\} \mathbf{H}^H = \sigma_\theta^2 \mathbf{H} \boldsymbol{\Lambda}_\theta \mathbf{H}^H = \sigma_s^2 \mathbf{R}_s$$

- \mathbf{U}_s is the $M \times r$ unitary matrix whose columns form the basis functions of the signal subspace.
- The subspace dimension is equal to the rank of \mathbf{R}_s , which is $r = \min([M \Delta \nu + 1], M)$.
- The target model coincides with the so-called Subspace Gaussian target model or Linear Gaussian model.



A Case Study: K-distributed Clutter

5

$$H_0 : \mathbf{z}_n = \mathbf{c}_n, \quad n = 1, 2, \dots, N \quad (N \text{ is the number of beams})$$

- The $M \times 1$ clutter vector at the output of the n th beamformer is:

$$\mathbf{c}_n = \sqrt{\tau_n} \mathbf{x}_n, \quad n = 1, 2, \dots, N$$

- Because the responses of the set of beamformers are orthogonal, i.e.

$$\mathbf{g}_n^H \mathbf{g}_k = N \cdot \delta[n - k]$$

the speckle vectors at the beamformer output can be assumed to be mutually orthogonal:

$$E\{\mathbf{x}_n \mathbf{x}_k^H\} = \mathbf{M} \delta[n - k]$$

- Derivation of the joint probability density function (PDF) of $\{\mathbf{z}_n\}$ when the N textures $\{\tau_n\}$ are partially correlated is infeasible. Hence, we assume here that the textures $\{\tau_n\}$ are IID.



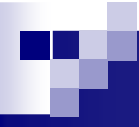
A Case Study: K-distributed Clutter

6

- In K-distributed clutter, the texture is Gamma distributed, with scale parameter μ and shape parameter ν :

$$p_\tau(\tau) = \frac{\tau^{\nu-1}}{\Gamma(\nu)} \left(\frac{\nu}{\mu} \right)^\nu \exp\left(-\frac{\nu\tau}{\mu}\right), \quad \tau \geq 0$$

- The disturbance power is $\sigma_d^2 = E\{\tau\} = \mu$
- Parameter ν is a measure of clutter spikiness, the lower ν the spikier the clutter.
- Gaussian clutter is obtained as a limit when $\nu \rightarrow \infty$ but the clutter may be considered Gaussian with good approximation for $\nu > 10$.
- When the clutter is K-distributed, the power of the thermal noise is supposed to be negligible with respect to the clutter power (this means that $CNR=\infty$).

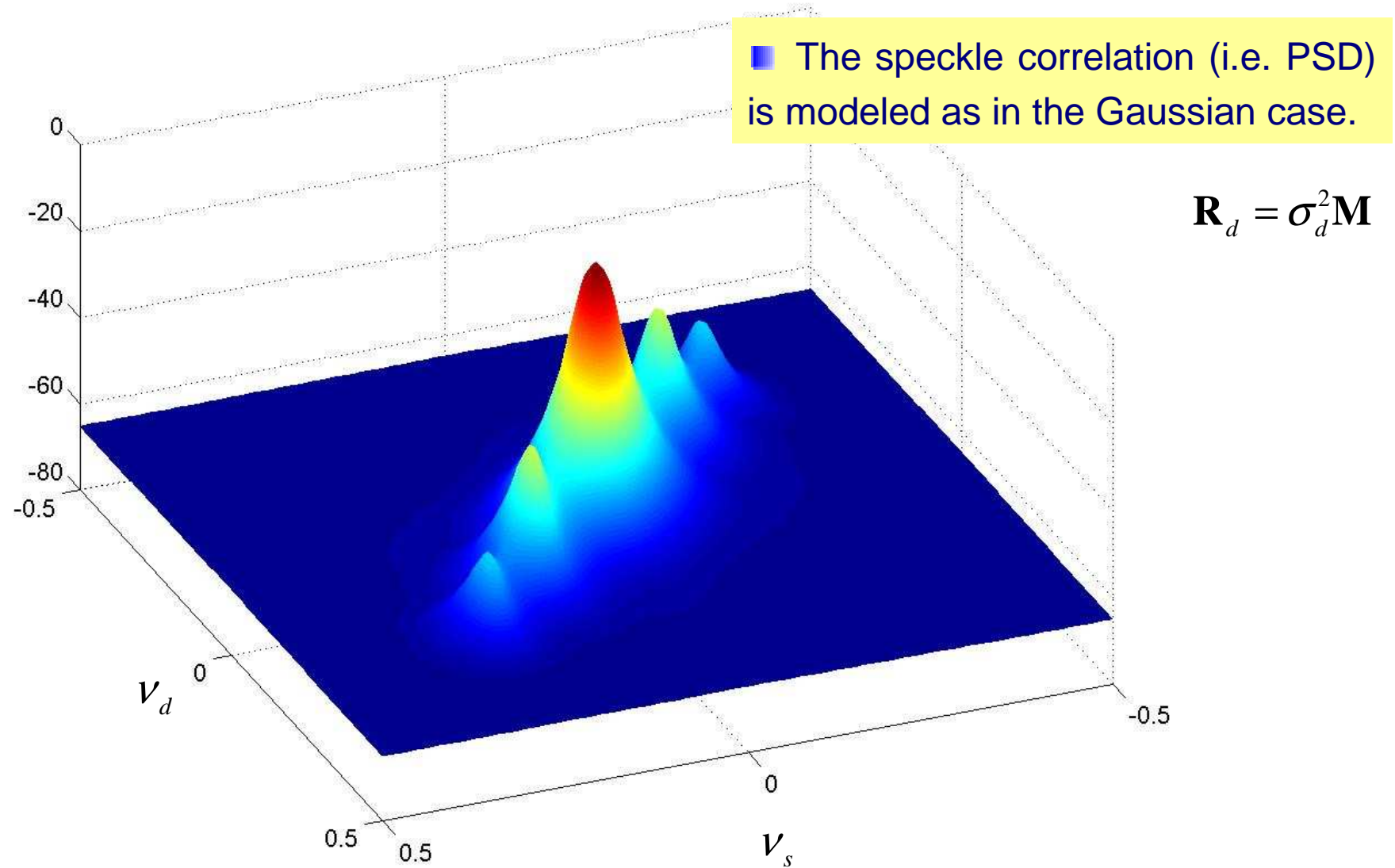


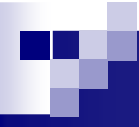
A Case Study: K-distributed Clutter

7

■ 2D speckle PSD [dB]

$$N = 10, M = 16, \alpha_c = 1$$



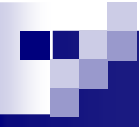


A Case Study: Subspace Gaussian Target

8

- The focus here is not on the DOA estimation problem but on the performance analysis and comparison of the detectors previously derived. Hence, we consider the output of a generic beamformer, say the one steered along direction of interrogation ψ_n .
- The output of the block labeled “ $\Lambda(\mathbf{z}_n)$ ” is compared to a threshold η and a decision is taken about the presence or the absence of the target signal in the n th beam.
- “ $\Lambda(\mathbf{z}_n)$ ” may represent in turn, the optimum NP detector, the GLRT detector, or the CFAR detector (the subscript K in the legend of the figures denotes the fact that we refer to the NP and GLRT detectors designed for K -distributed clutter, the CFAR detector does not have a subscript because it is the same for Gaussian clutter and compound-Gaussian clutter).

$$\text{Signal-to-total Disturbance Power Ratio : } SDR = \frac{\sigma_s^2}{\sigma_d^2} = \frac{\sigma_s^2}{\mu}$$



Subspace Detectors in Gaussian Clutter

9

Target	Clutter	Detector	Comments
Gaussian	Gaussian	$\mathbf{z}^H \mathbf{Q}_1 \mathbf{z} \stackrel{H_1}{\underset{H_0}{>}} \eta$	NP: quadratic in \mathbf{z}
Unknown deterministic (or random with unknown pdf)	Gaussian	$\mathbf{z}^H \mathbf{Q}_2 \mathbf{z} \stackrel{H_1}{\underset{H_0}{>}} \eta$	GLRT: quadratic in \mathbf{z}
Unknown deterministic (or random with unknown pdf)	Gaussian with unknown power	$\frac{\mathbf{z}^H \mathbf{Q}_2 \mathbf{z}}{\mathbf{z}^H \mathbf{M}^{-1} \mathbf{z}} \stackrel{H_1}{\underset{H_0}{>}} \eta$	CFAR: ratio of two quadratic forms in \mathbf{z}

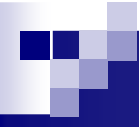
$$\mathbf{s}_t = \mathbf{H}\boldsymbol{\theta}, \quad \mathbf{R}_t = E\{\mathbf{s}_t \mathbf{s}_t^H\} = \mathbf{H}E\{\boldsymbol{\theta} \boldsymbol{\theta}^H\} \mathbf{H}^H = \sigma_\theta^2 \mathbf{H} \boldsymbol{\Lambda}_\theta \mathbf{H}^H = \sigma_s^2 \mathbf{R}_s$$

$$\mathbf{R}_d = \sigma_d^2 \mathbf{M}, \quad SDR = \sigma_s^2 / \sigma_d^2$$

$$\mathbf{Q}_1 = \mathbf{M}^{-1} - (\mathbf{M} + SDR \cdot \mathbf{R}_s)^{-1}$$

$$\mathbf{Q}_2 = \mathbf{M}^{-1} \mathbf{H} (\mathbf{H}^H \mathbf{M}^{-1} \mathbf{H})^{-1} \mathbf{H}^H \mathbf{M}^{-1}$$

■ The GLRT and CFAR detectors do not require a-priori knowledge of SDR .

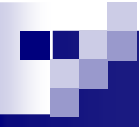


Subspace Detectors in Compound-Gaussian Clutter

10

Target	Clutter	Detector	Comments
Gaussian	compound-Gaussian	$\frac{\int_0^{\infty} \frac{1}{ \sigma_s^2 \mathbf{R}_s + \tau \mathbf{M} } \exp\left(-\mathbf{z}^H (\sigma_s^2 \mathbf{R}_s + \tau \mathbf{M})^{-1} \mathbf{z}\right) p_\tau(\tau) d\tau}{\int_0^{\infty} \frac{1}{\tau^m \mathbf{M} } \exp\left(-\frac{\mathbf{z}^H \mathbf{M}^{-1} \mathbf{z}}{\tau}\right) p_\tau(\tau) d\tau} \stackrel{H_1}{\underset{H_0}{>}} \eta$	NP: nonlinear and quadratic in \mathbf{z} (high computational load)
Unknown deterministic (or random with unknown pdf)	compound-Gaussian	$\mathbf{z}^H \mathbf{Q}_2 \mathbf{z} \stackrel{H_1}{\underset{H_0}{>}} f(q_0(\mathbf{z}), \eta)$ <p style="text-align: center;">with $q_0(\mathbf{z}) = \mathbf{z}^H \mathbf{M}^{-1} \mathbf{z}$</p>	GLRT: quadratic in \mathbf{z} with data-dependent threshold
Unknown deterministic (or random with unknown pdf)	compound-Gaussian	$\mathbf{z}^H \mathbf{Q}_2 \mathbf{z} \stackrel{H_1}{\underset{H_0}{>}} f_{approx}(q_0(\mathbf{z}), \eta)$	$f_{approx}(\cdot)$ is an approximation of the optimal $f(\cdot)$
Unknown deterministic (or random with unknown pdf)	compound-Gaussian, with unknown texture pdf	$f_{approx}(\cdot) = f_{ML}(\cdot) = \eta q_0(\mathbf{z}) \Rightarrow \frac{\mathbf{z}^H \mathbf{Q}_2 \mathbf{z}}{\mathbf{z}^H \mathbf{M}^{-1} \mathbf{z}} \stackrel{H_1}{\underset{H_0}{>}} \eta$	CFAR: ratio of two quadratic forms in \mathbf{z}

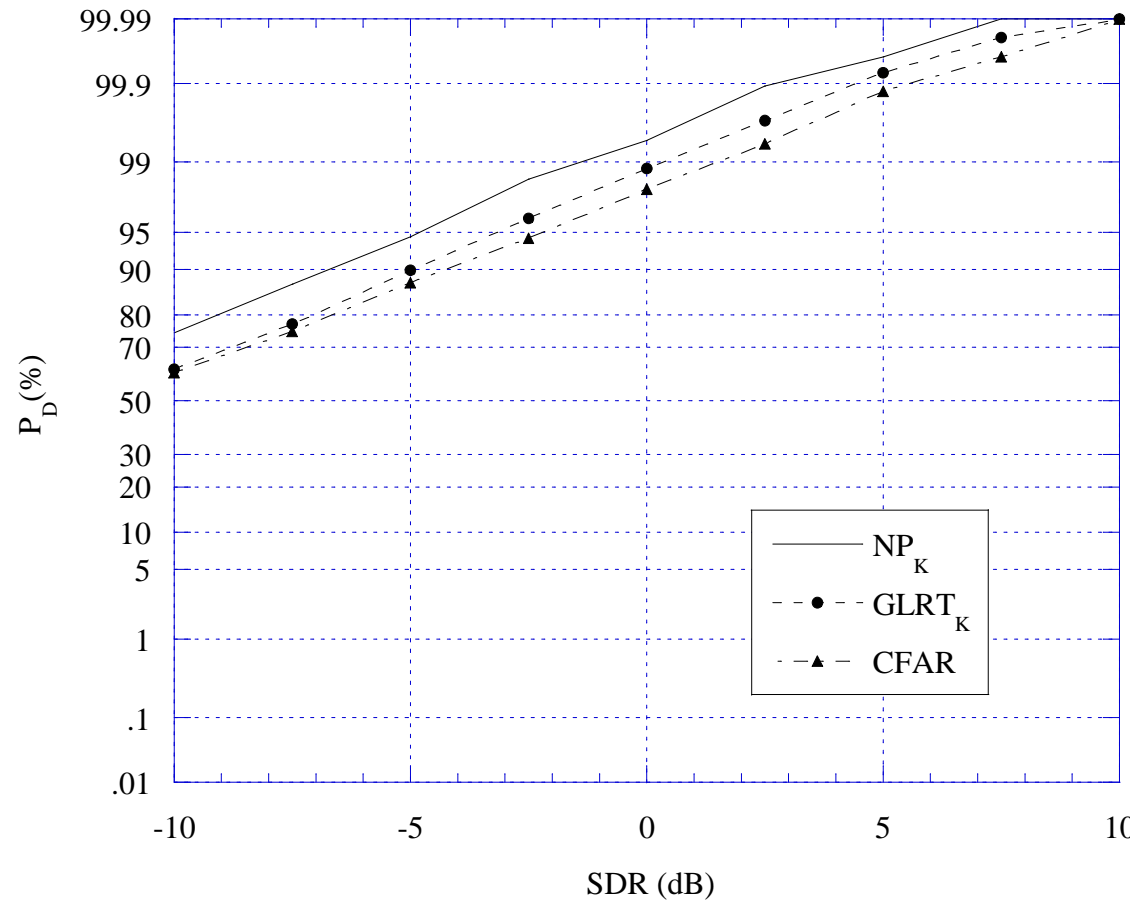
- In Gaussian clutter the threshold is constant η , in CG it is a nonlinear function of the quadratic statistic q_0 .



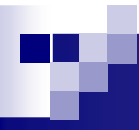
A Case Study: Subspace Gaussian Target

11

■ Probability of detection versus the signal-to-total-disturbance power ratio



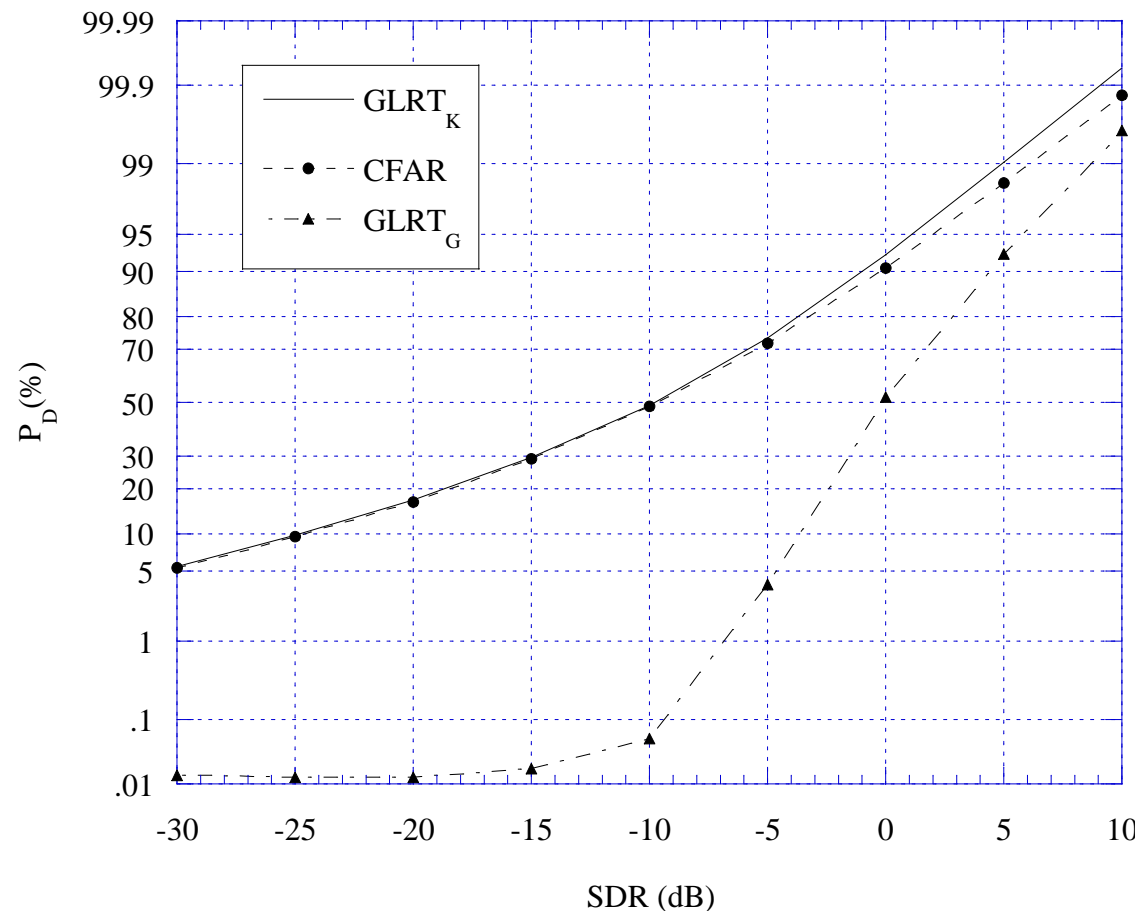
$$P_{FA} = 10^{-2}, \#MC \text{ runs} = 10^5, N = 10, M = 16, \nu_0 = 0, \Delta\nu = 0.2, r = 5, \nu = 1.5, CNR = +\infty$$



A Case Study: Subspace Gaussian Target

12

■ Probability of detection versus the signal-to-total-disturbance power ratio

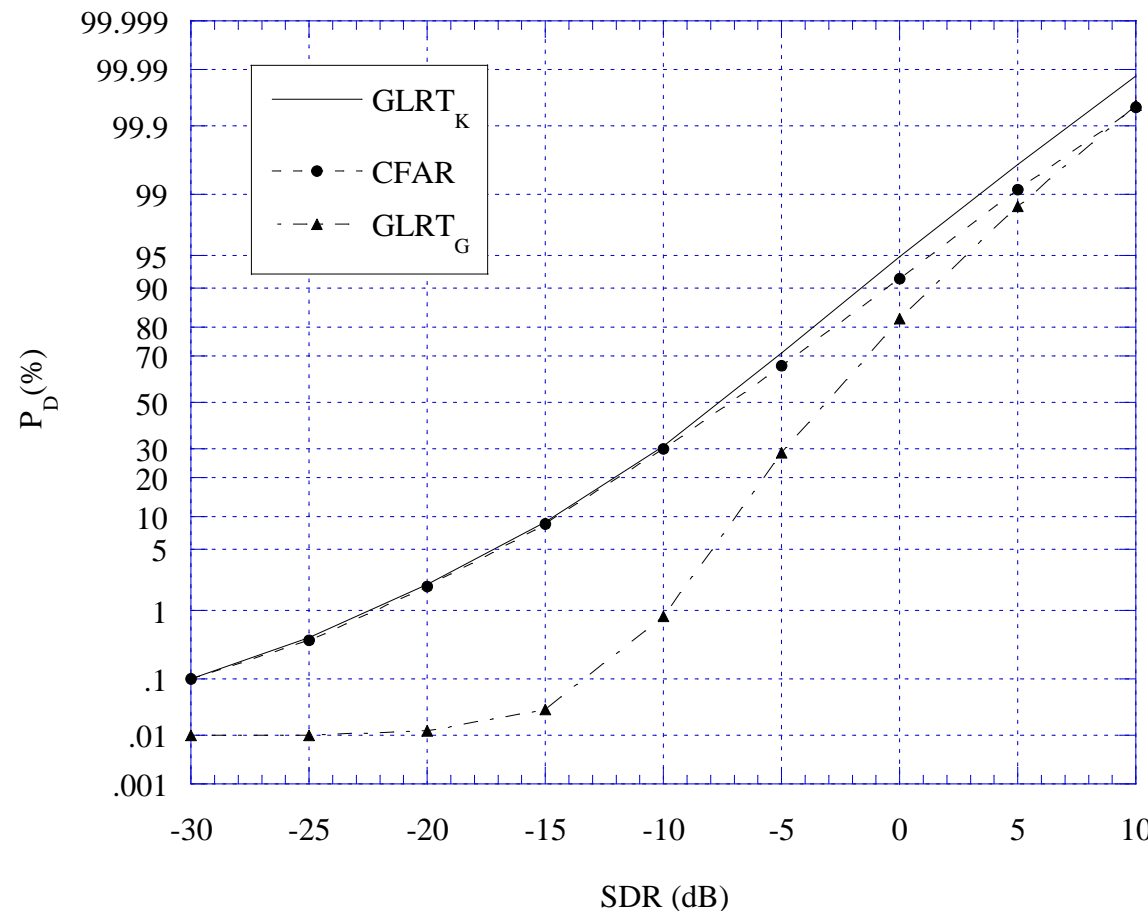


$$P_{FA} = 10^{-4}, \#MC \text{ runs} = 10^5, N = 10, M = 16, \nu_0 = 0, \Delta\nu = 0.2, r = 5, \nu = 0.5, CNR = +\infty$$

A Case Study: Subspace Gaussian Target

13

■ Probability of detection versus the signal-to-total-disturbance power ratio

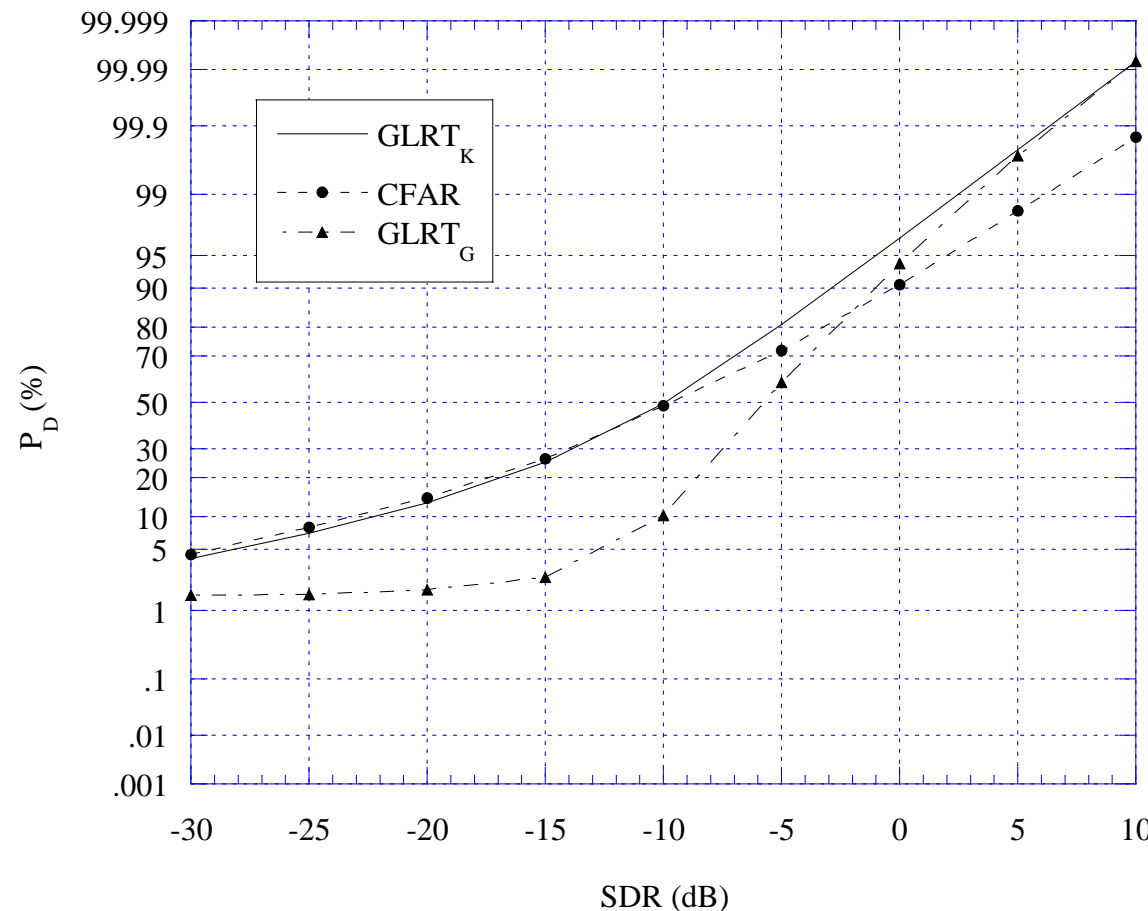


$$P_{FA} = 10^{-4}, \#MC \text{ runs} = 10^5, N = 10, M = 16, \nu_0 = 0, \Delta\nu = 0.2, r = 5, \nu = 1.5, CNR = +\infty$$

A Case Study: Subspace Gaussian Target

14

■ Probability of detection versus the signal-to-total-disturbance power ratio

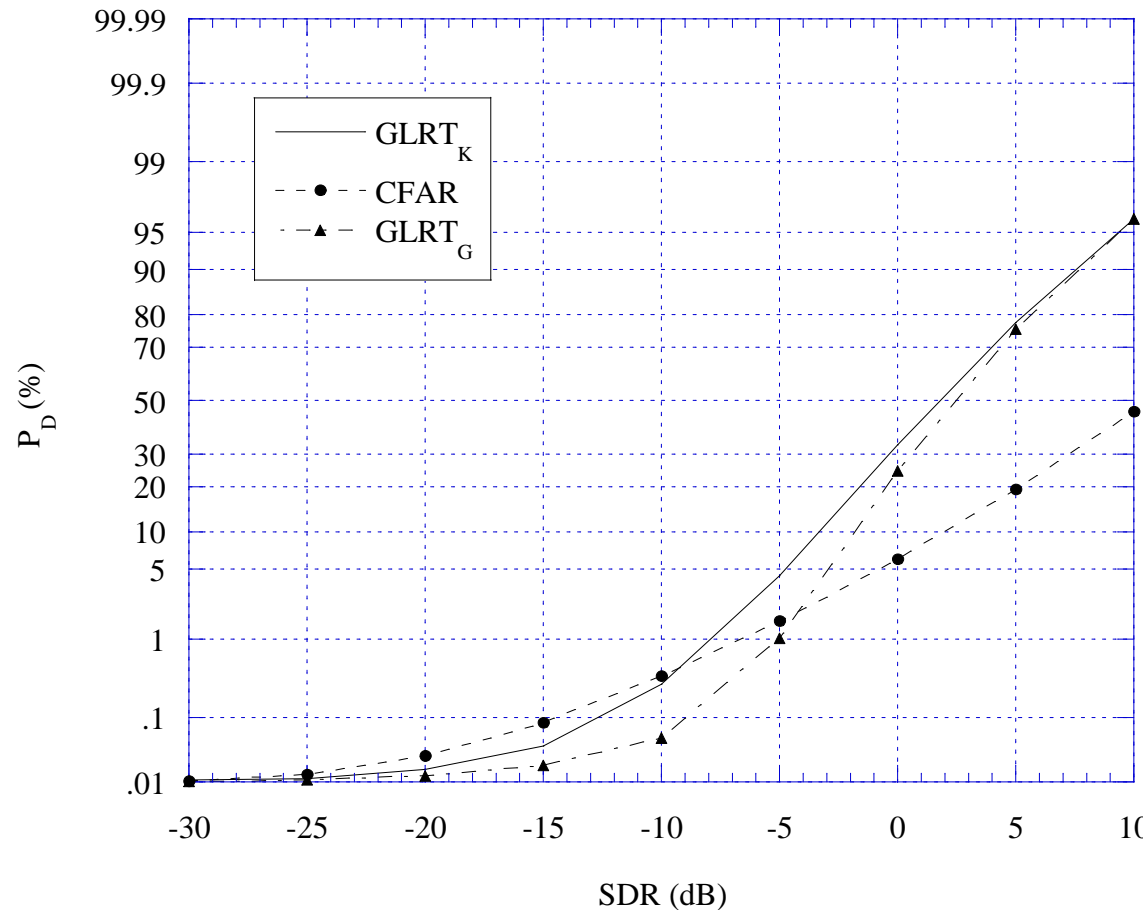


$$P_{FA} = 10^{-4}, \#MC \text{ runs} = 10^5, N = 10, M = 16, \nu_0 = 0, \Delta\nu = 0.2, r = 5, \nu = 4.5, CNR = +\infty$$

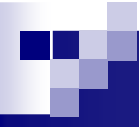
A Case Study: Subspace Gaussian Target

15

- Probability of detection versus the signal-to-total-disturbance power ratio



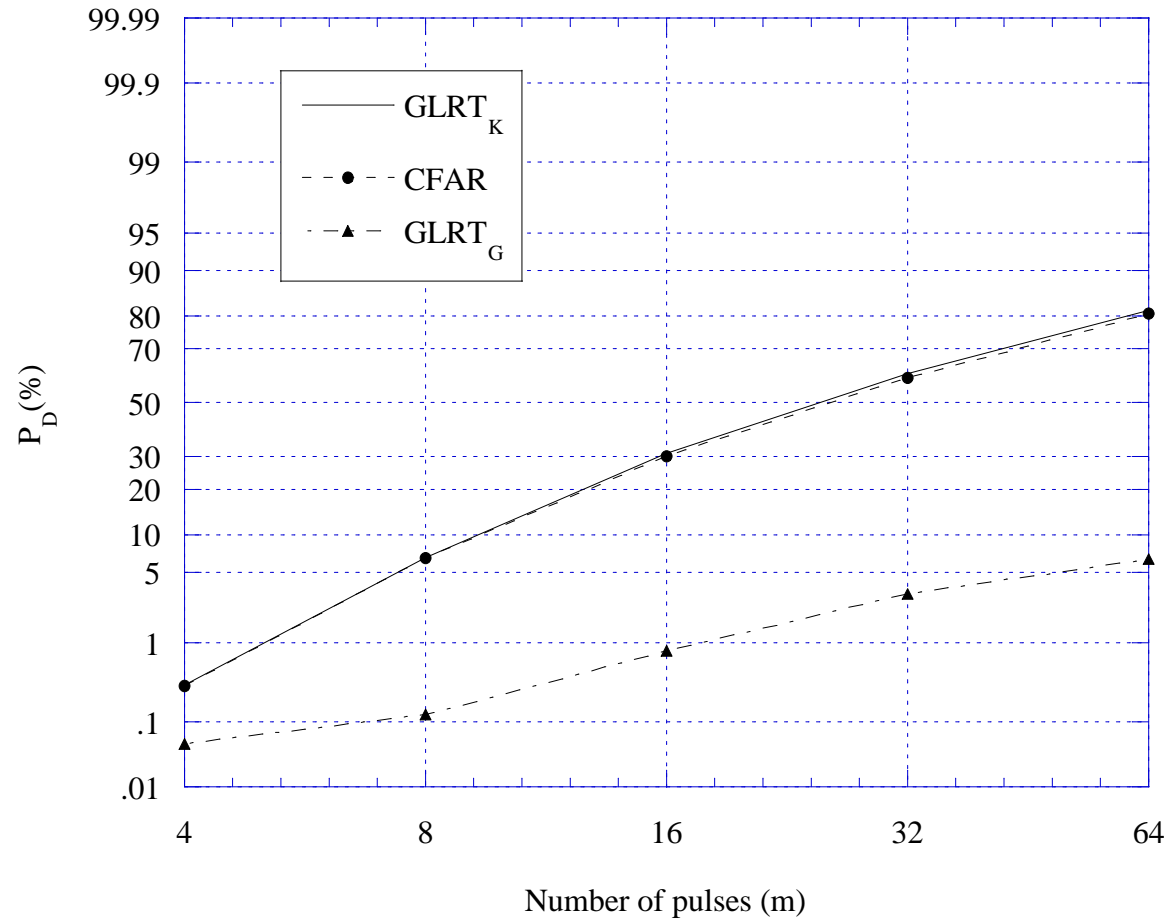
$$P_{FA} = 10^{-4}, \#MC \text{ runs} = 10^5, N = 10, M = 4, \nu_0 = 0, \Delta\nu = 0.2, r = 5, \nu = 1.5, CNR = +\infty$$



A Case Study: Subspace Gaussian Target

16

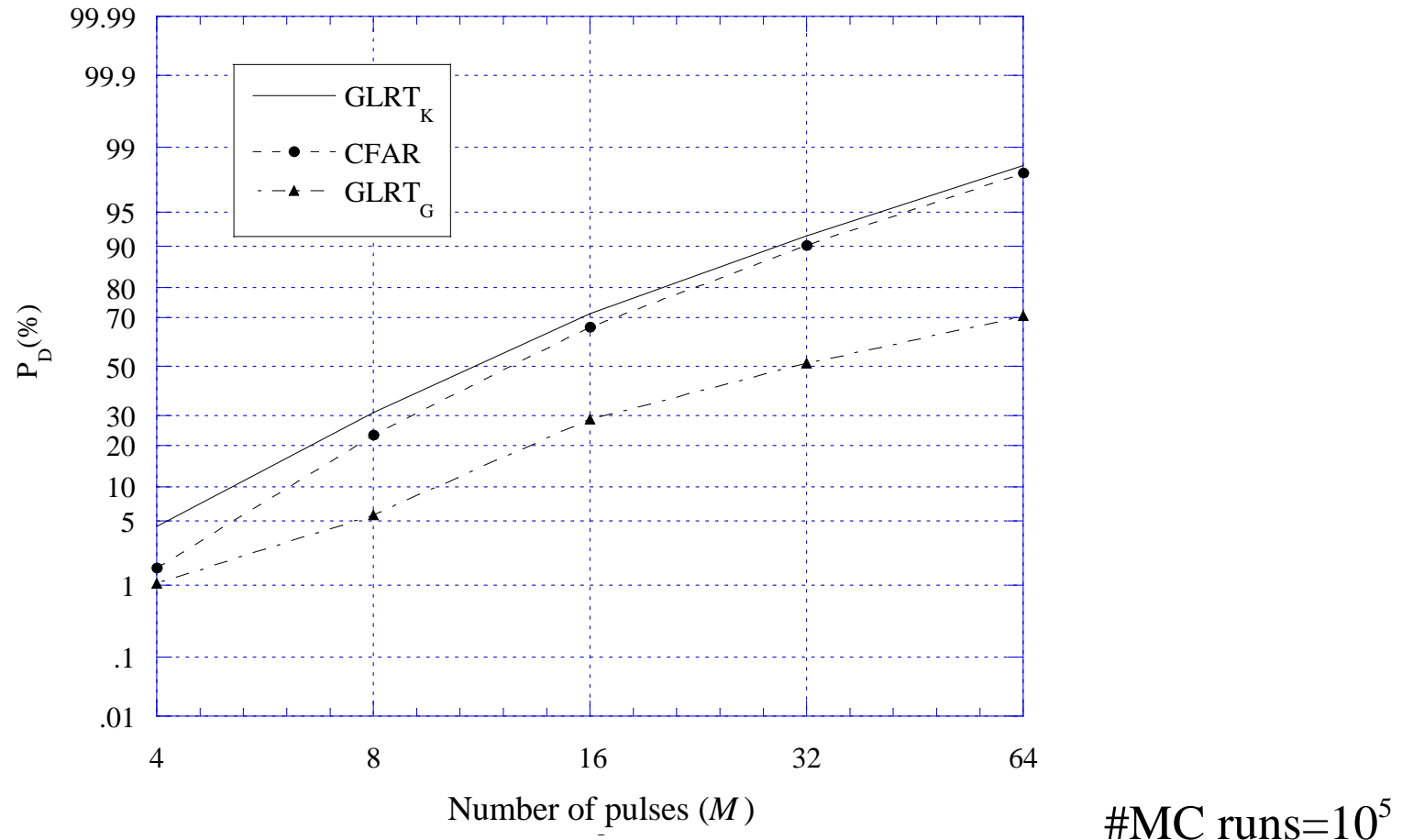
■ Probability of detection versus the number of pulses M



#MC runs = 10^5

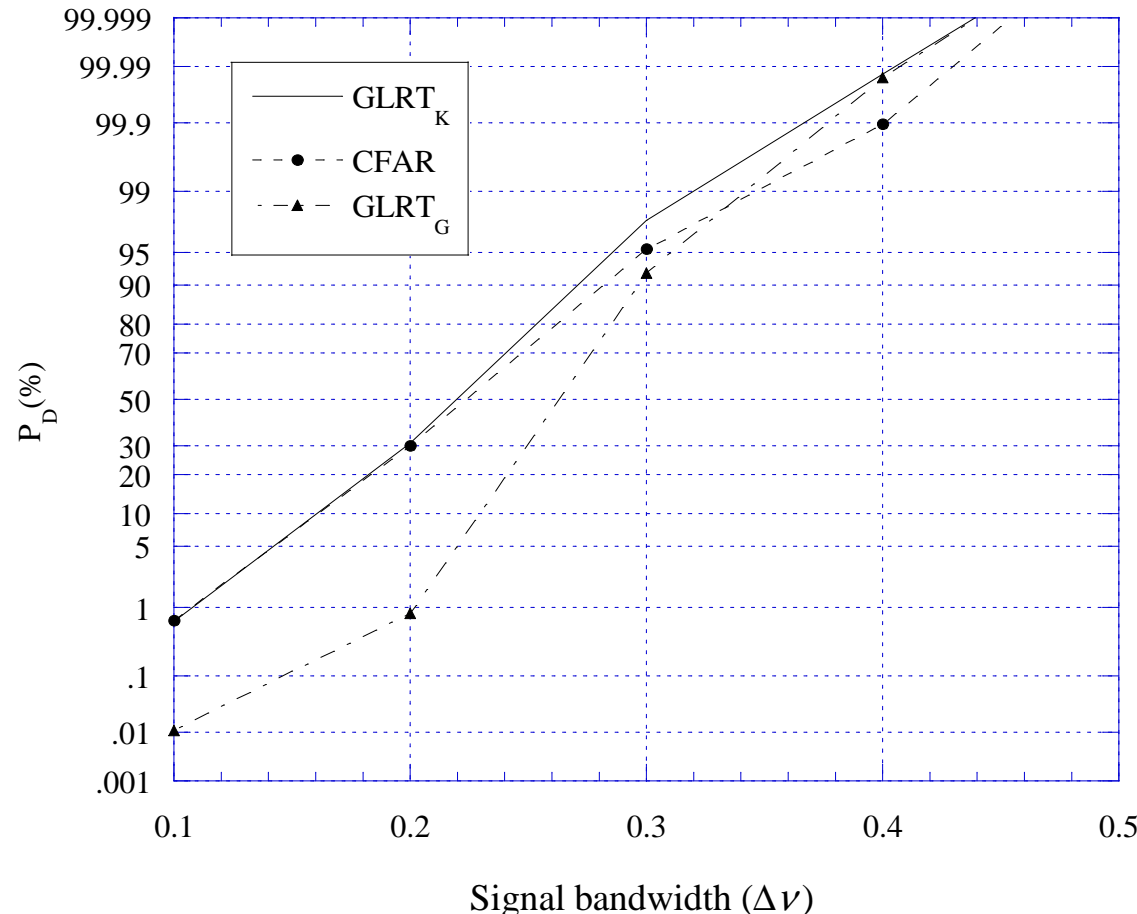
$$P_{FA} = 10^{-4}, N = 10, \nu_0 = 0, \Delta\nu = 0.2, r = 5, SDR = -10 \text{ dB}, \nu = 1.5, CNR = +\infty$$

■ Probability of detection versus the number of pulses M

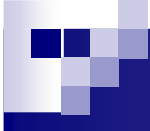


$$P_{FA} = 10^{-4}, N = 10, \nu_0 = 0, \Delta\nu = 0.2, r = 5, SDR = -5 \text{ dB}, \nu = 1.5, CNR = +\infty$$

■ Probability of detection versus the target signal bandwidth $\Delta\nu$



$$P_{FA} = 10^{-4}, \#MC \text{ runs} = 10^5, N = 10, M = 16, \nu_0 = 0, SDR = -10 \text{ dB}, \nu = 1.5, CNR = +\infty$$

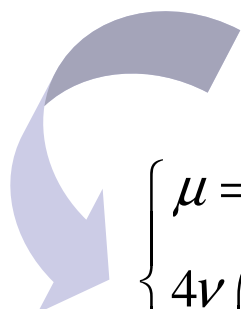


A Case Study: Subspace Gaussian Target

19

- To analyze how the possible ignorance of the texture parameters μ and ν may affect the performance of the GLRT_K detector, we also considered the case where they are unknown and must be estimated from the data.
- We estimated them from L secondary target-free independent and identically distributed (i.i.d.) data vectors $\{\mathbf{z}_i, i=1,2, \dots, L\}$ coming from close range bins.
- The estimation algorithm is based on the method of moments, which amounts to equate the moments of the clutter amplitude $R=|z|$ with the theoretical moments and solve with respect to the unknown parameters.
- The moments of the K-distribution are given by:

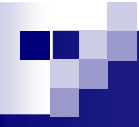
$$m_R[k] = E\{R^k\} = \left(\frac{\mu}{\nu}\right)^{k/2} \frac{\Gamma(k/2 + \nu)\Gamma(k/2 + 1)}{\Gamma(\nu)}, \quad k \geq 1$$



$$\begin{cases} \mu = m_R[2] \\ \frac{4\nu}{\pi} \left(\frac{\Gamma(\nu)}{\Gamma(\nu + 1/2)} \right)^2 = \frac{m_R[2]}{m_R^2[1]} \end{cases}$$

The moments of the clutter amplitude are replaced by their sample estimates:

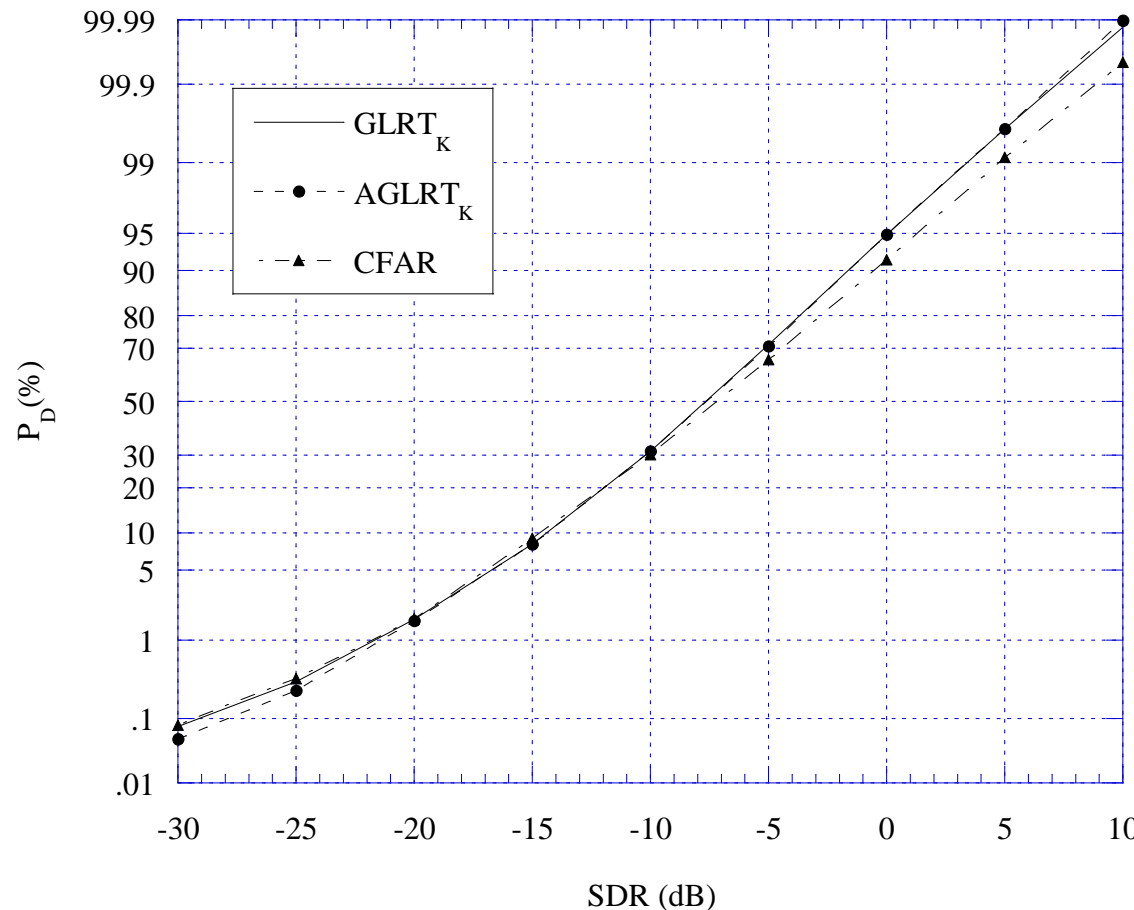
$$\hat{m}_R[k] = \frac{1}{ML} \sum_{n=1}^M \sum_{i=1}^L \|z_i[n]\|^k \rightarrow m_R[k]$$



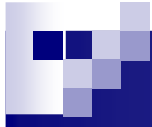
A Case Study: Subspace Gaussian Target

20

- This detector which adaptively estimates the clutter amplitude parameters is referred to as the adaptive GLRT (AGLRT).



$$L = 32, P_{FA} = 10^{-4}, N = 10, M = 16, \nu_0 = 0, \Delta\nu = 0.2, \nu = 1.5, CNR = +\infty$$



PERFORMANCE AGAINST MEASURED HIGH RESOLUTION SEA CLUTTER DATA

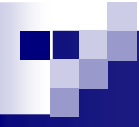
- The behavior of the GLRT and CFAR detectors is investigated by processing measured high resolution sea clutter data.
- The sea clutter data were collected at Osborne Head Gunnery Range (OHGR) in November 1993, with McMaster University IPIX X-band radar.
- IPIX is an experimental instrumentation class search radar, capable of dual polarized and frequency agile operation.
- There are always like polarizations, HH and VV (Lpol), and cross polarizations, HV and VH (Xpol), coherent reception, leading to a quadruplet of I and Q values for Lpol and Xpol.
- The experimental results reported here correspond to the VV case.
- The values of the main system and environmental parameters are reported in following Table.



File	Starea4
sea state	3
wind direct.	40 degrees
wind speed	22 Km/h
wave period	5 s
wave height	1.42 m
grazing angle	0.3 degrees
azimuth	78 degrees
PRF	2 KHz
Frequency	9.4 GHz
No. of frequencies	16
range resolution	30 m
No. of cells	7
start range	1800 m
samples/cell	131072
beam width	≈ 1 degrees

System and environmental parameters²

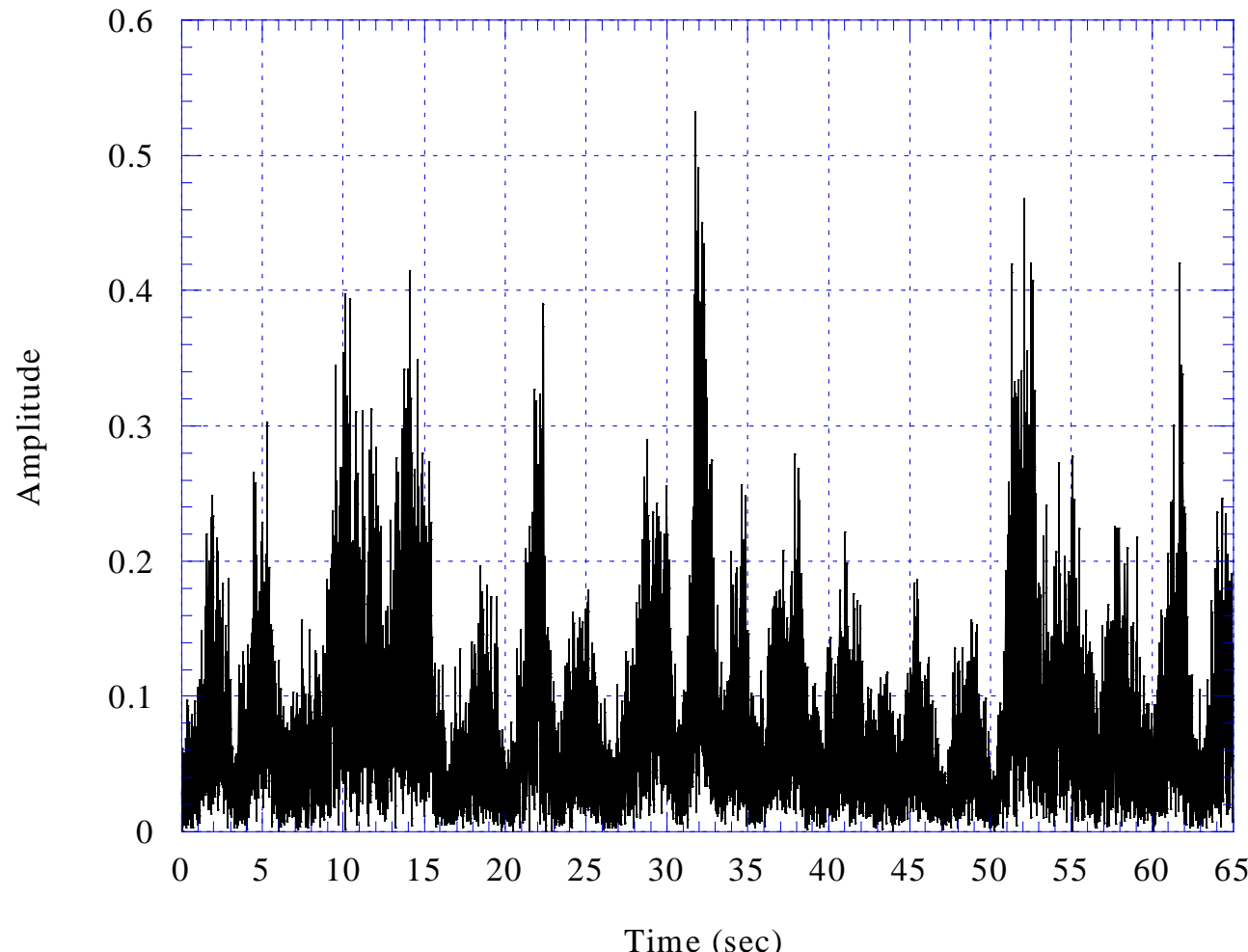
- Note that the grazing angle is quite low, 0.3° , so we expect a non-Gaussian behavior of the clutter statistics; while the range resolution is 30 m, so we expect the speckle to be Gaussian distributed (there is a lower bound in the resolution cell area for the speckle PDF to be Gaussian distributed. This bound was estimated to be 120 m in azimuth resolution and 4 m in range resolution).
- Preliminary statistical analyses have shown that the data are well modeled by a K-distribution.



A Case Study: Subspace Gaussian Target

23

- The clutter amplitude in the 1° rang cell is plotted for a time interval of 65 s. The highly spiky nature of the clutter is well evident.



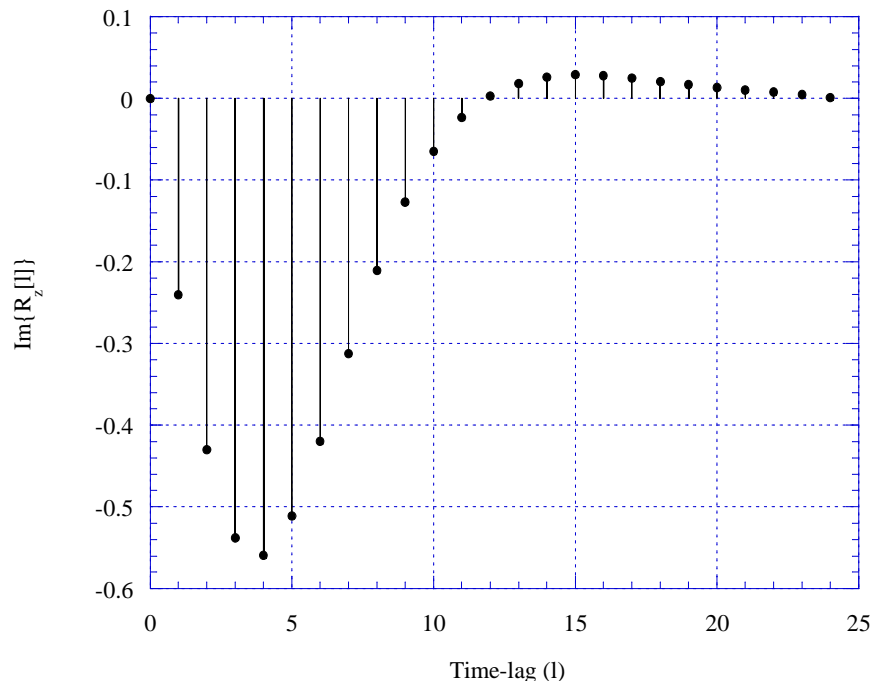
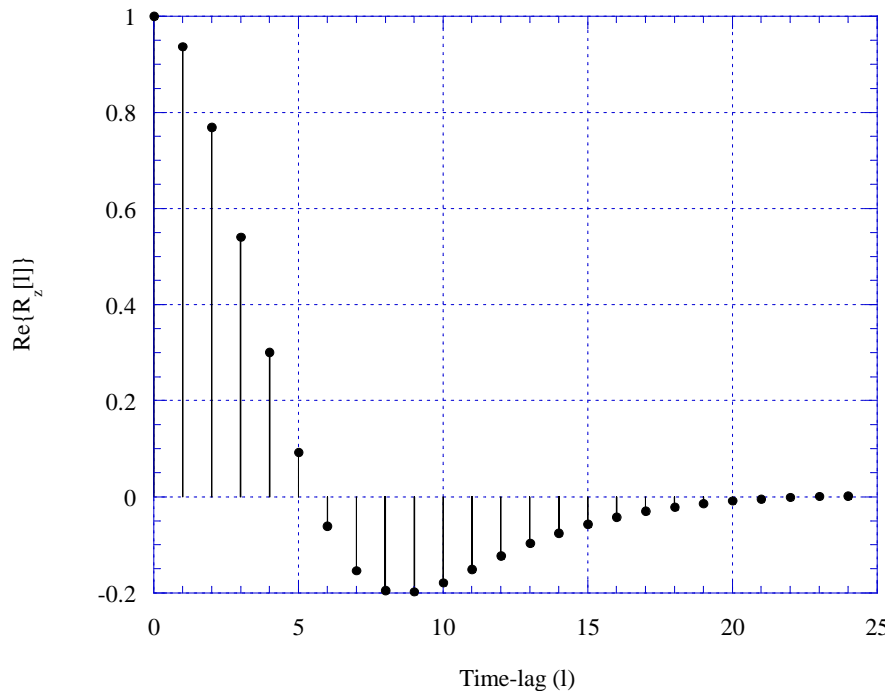
A Case Study: Subspace Gaussian Target

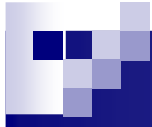
24

- The data ACF was estimated from all the available data (for each range bin):

$$\hat{r}[l] = \frac{1}{M-l} \sum_{n=0}^{M-l-1} z^*[n]z[n+l]$$

- The decorrelation time is estimated to be around 12.5 ms.





A Case Study: Subspace Gaussian Target

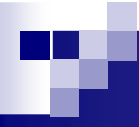
25

- The texture parameters are estimated with the method of moments:

$$1st \text{ range cell: } \hat{\nu} = 1.1105, \quad \hat{\mu} = 8.7 \cdot 10^{-3}$$

$$4th \text{ range cell: } \hat{\nu} = 1.2694, \quad \hat{\mu} = 8.7 \cdot 10^{-3}$$

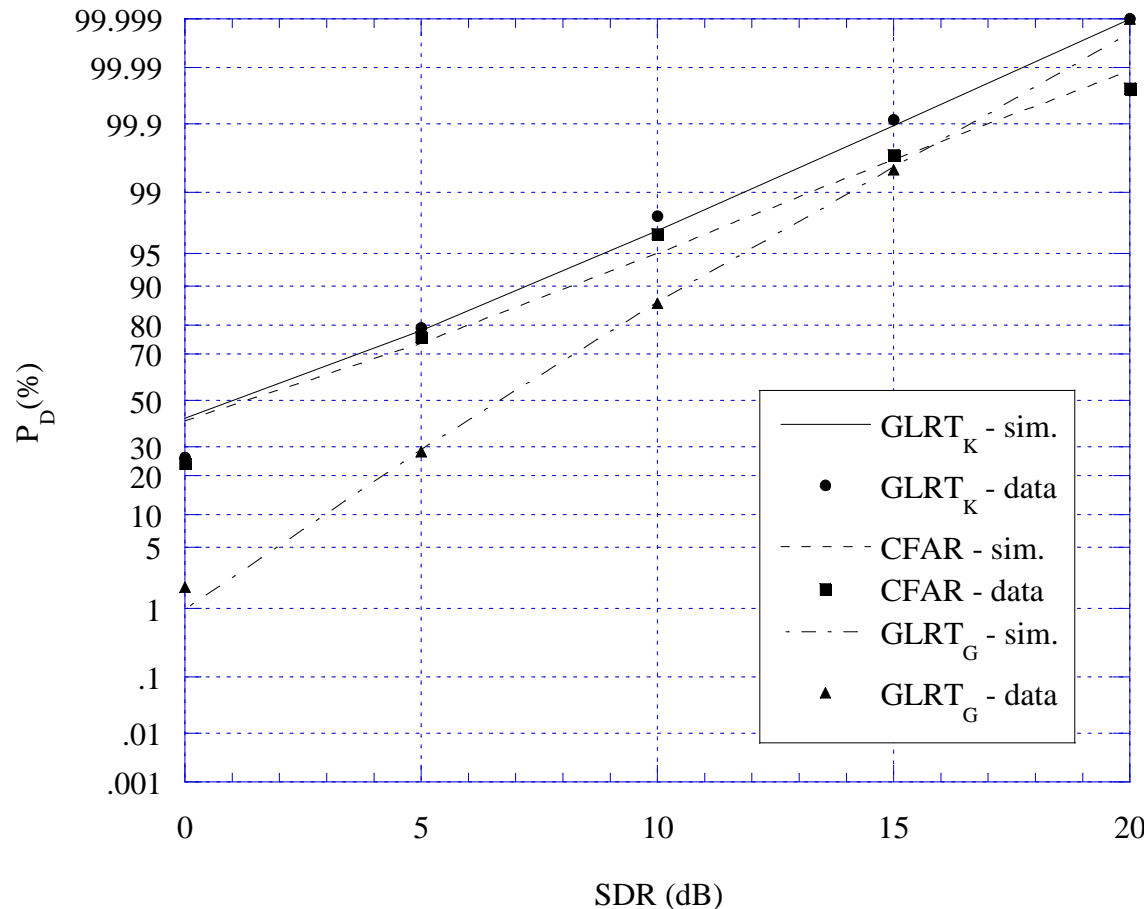
- We used all the available data from each range bin.
- To estimate the detection performance, a synthetic target was added to the measured clutter data.
- The detection algorithms were tested both on the measured sea clutter data and on the data generated by computer simulation having the same statistical properties of the measured clutter, i.e., we generated K-distributed clutter with ACF equal to the estimated ACF and ν and μ equal to the estimated texture parameters.
- The numerical results should be close as far as the compound Gaussian model with K-distributed amplitude is an accurate model of the measured sea clutter data (and the clutter data are homogeneous).



A Case Study: Subspace Gaussian Target

26

- Probability of detection versus the signal-to-total-disturbance ratio, real sea clutter data (1st range bin).

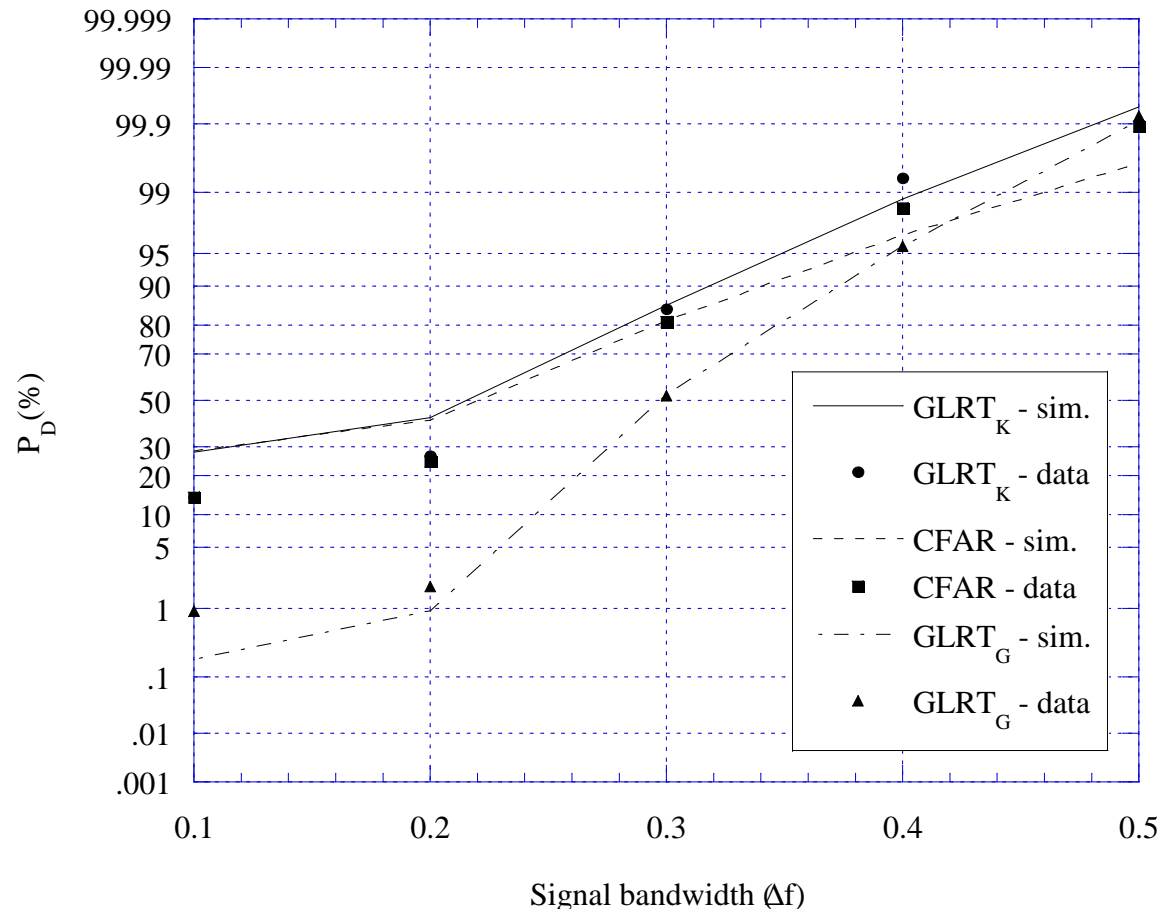


$$\hat{\nu} = 1.1105, \hat{\mu} = 8.7 \cdot 10^{-3}, M = 16, \nu_0 = 0, \Delta\nu = 0.2, P_{FA} = 10^{-4}$$

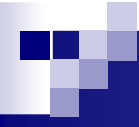
A Case Study: Subspace Gaussian Target

27

- Probability of detection versus the target signal bandwidth, real sea clutter data (1st range bin).



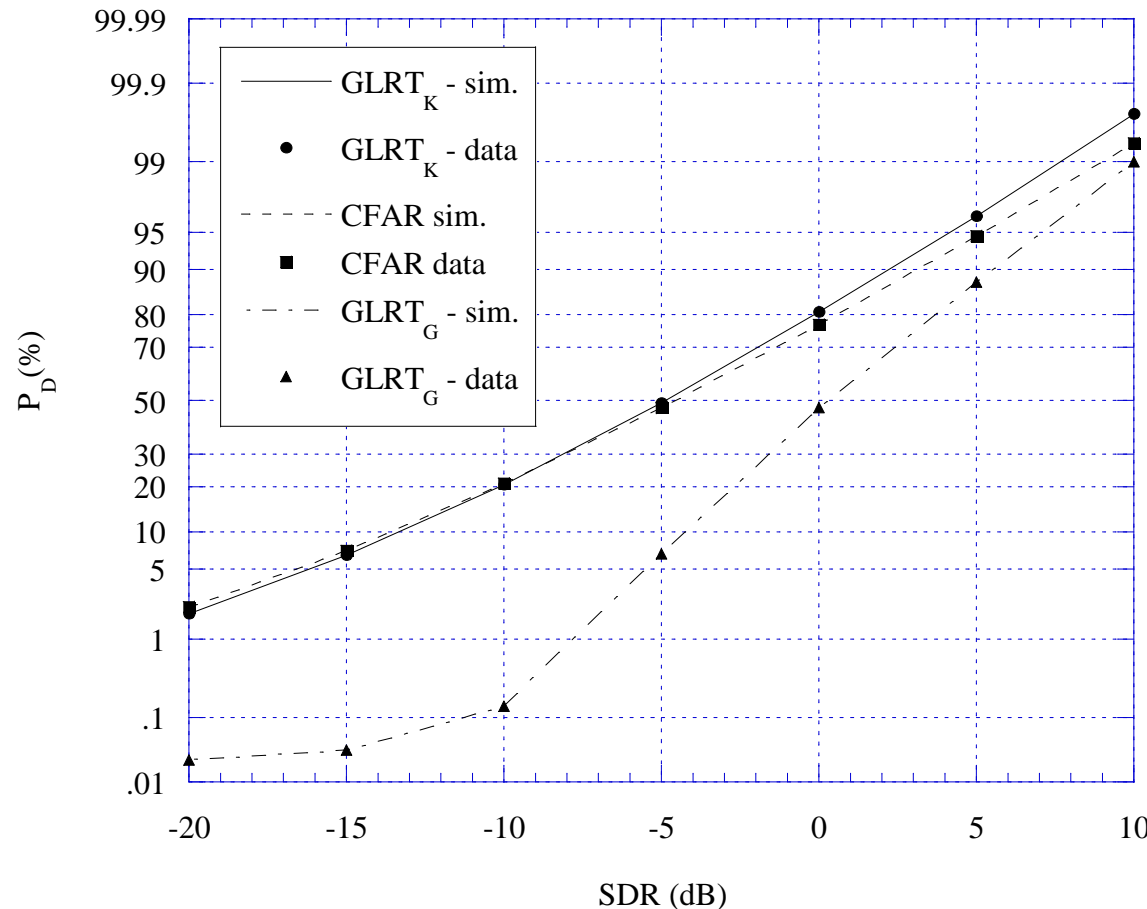
$$\hat{\nu} = 1.1105, \hat{\mu} = 8.7 \cdot 10^{-3}, M = 16, \nu_0 = 0, P_{FA} = 10^{-4}, SDR = 0 dB$$



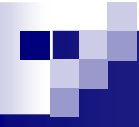
A Case Study: Subspace Gaussian Target

28

- Probability of detection versus the signal-to-total-disturbance ratio, real sea clutter data (4th range bin).



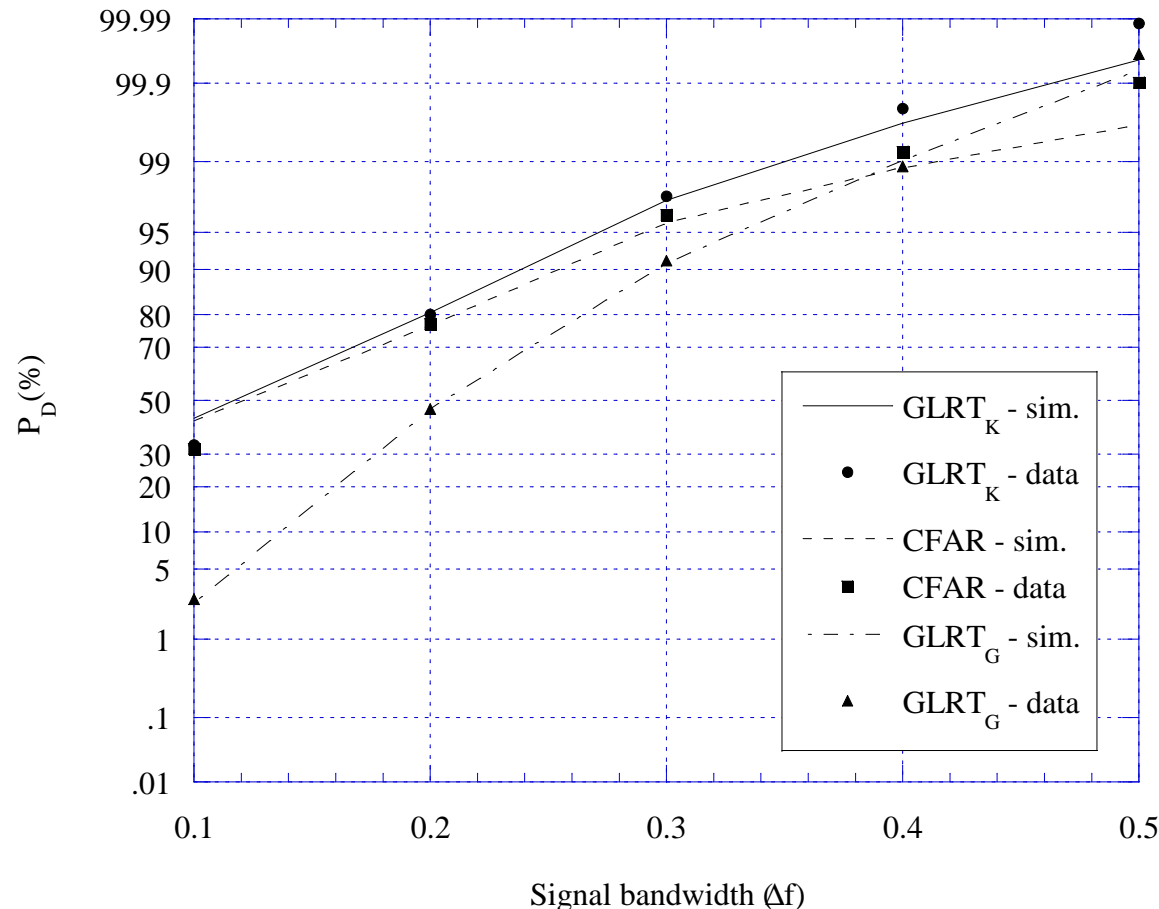
$$\hat{\nu} = 1.2694, \hat{\mu} = 8.7 \cdot 10^{-3}, M = 16, \nu_0 = 0, \Delta\nu = 0.2, P_{FA} = 10^{-4}$$



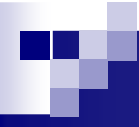
A Case Study: Subspace Gaussian Target

29

- Probability of detection versus the target signal bandwidth, real sea clutter data (4th range bin).

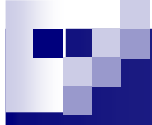


$$\hat{\nu} = 1.2694, \hat{\mu} = 8.7 \cdot 10^{-3}, M = 16, \nu_0 = 0, P_{FA} = 10^{-4}, SDR = 0 \text{ dB}$$



Some remarks:

- All the numerical results show a good agreement between measured and simulated data, thus validating the compound Gaussian model for these high resolution sea clutter data.
- The numerical results shown here allow to find the best trade-off between computational complexity and detection performance for various detection scenarios.
- As the number of pulses to be processed increases, the CFAR detector, (remember that for rank-1 signal it becomes the NMF), which does not require information about the specific nature of the non-Gaussian clutter, may be implemented to obtain quasi-optimal performance.
- The quasi-optimality of the CFAR is shown to be a consequence of the fact that for large numbers of pulses, the maximum likelihood estimate of $\tau=1/\alpha$ is quasi-optimal (it is asymptotically optimal but already for $M=16$ we are in the asymptotic regime).



A Case Study: Subspace Gaussian Target

31

- More details on the problem of detecting a subspace Gaussian target in Gaussian and compound-Gaussian clutter can be found in:
- F. Gini and A. Farina, “Matched Subspace CFAR Detection of Hovering Helicopters,” *IEEE Trans. on Aerospace and Electronic Systems*, vol. 35, No. 4, pp. 1293-1305, October 1999.
- F. Gini, A. Farina, “Vector Subspace Detection in Compound-Gaussian Clutter. Part I: Survey and New Results,” *IEEE Trans. on Aerospace and Electronic Systems*, Vol. 38, No. 4, pp. 1295-1311, October 2002.
- F. Gini, A. Farina, M. Montanari, “Vector Subspace Detection in Compound-Gaussian Clutter. Part II: Performance analysis,” *IEEE Trans. on Aerospace and Electronic Systems*, Vol. 38, No. 4, pp. 1312-1323, October 2002.